Collagen from the Osteogenesis Imperfecta Mouse Model (oim) Shows Reduced Resistance Against Tensile Stress

K. Misof,*‡ W.J. Landis,§ K. Klaushofer,‡ and P. Fratzl*‡

**Institut für Materialphysik der Universität Wien A-1090 Wien, Austria; ‡Ludwig Boltzmann-Institut für Osteologie, Hanusch Krankenhaus, A-1140 Wien, Austria; and §Department of Orthopedic Surgery, Harvard Medical School and Children's Hospital, Boston, Massachusetts 02115*

Abstract

Osteogenesis imperfecta (OI) is a disease attributable to any of a large number of possible mutations of type I collagen. The disease is clinically characterized in part by highly brittle bone, the cause of this feature being unknown. Recently a mouse model of OI, designated as osteogenesis imperfecta murine (oim), and having a well defined genetic mutation, has been studied and found to contain mineral crystals different in their alignment with respect to collagen and in their size. These observations are consistent with those reported in human OI and the unusual crystal alignment and size undoubtedly contribute to the reduced mechanical properties of OI bone. While the mineral has been investigated, no information is available on the tensile properties of oim collagen. In this study, the mechanical properties of tendon collagen under tension have been examined for homozygous (oim/oim), heterozygous (+/oim), and control (+/+) mice under native wet conditions. The ultimate stress and strain found for oim/oim collagen were only about half the values for control mice. Assuming that prestrained collagen molecules carry most of the tensile load in normal bone while the mineral confers rigidity and compression stability, the reported results suggest that the brittleness of OI bone in the mouse model may be related to a dramatic reduction of the ultimate tensile strain of the collagen. (*J. Clin. Invest.* 1997. 100:40–45.) Key words: collagen • osteogenesis imperfecta • mechanical properties • stress/strain • x-ray scattering

Introduction

Osteogenesis imperfecta (OI)[1] (Brittle Bone Syndrome) is a disease which results from a variety of mutations in type I collagen (1, 2). Phenotypically, the disease presents a broad spectrum of effects (3, 4). Bone brittleness is the hallmark of all types of OI, but in many cases structural and functional alterations of the teeth, skin, and the sclera of the eyes occur as well (5). The origin of the brittleness of bone and changes in other tissues are not yet clear. Bone itself is a complicated composite combining very hard and brittle material, the mineral, with much softer material, the collagen fibrils (6). The collagen fibrils are the tension elements and the mineral is responsible for stiffness against compression. In addition to the combination of these two very different components, the hierarchical structure of bone optimizes the composite material from the nanometer scale to the macroscopic scale. Some abnormalities in the composite material, including the presence of both hypo- or hypermineralized regions (1) and changes in collagen cross-links (7), mineral crystallinity (7), and collagen fibril diameters (8), have been suggested as possible sources for the brittleness of OI bone.

Recently the osteogenesis imperfecta mouse model (oim), which has a well defined genetic mutation, has become available for the study of increased bone brittleness typical of human OI (9). The homozygous oim mouse produces only α1(I) collagen. This leads to an abnormal collagen molecule comprised of three α1(I) chains rather than the normal two α1(I) and one α2(I) chains. Such molecules still form a helical structure but increased bone brittleness is observed (9), which models the situation in human OI (10). Recent small angle x-ray scattering (SAXS) studies of the nanometer level of oim bone structure have shown that the crystals were thinner and less well oriented than in the counterpart normal mouse bone. These differences in the nature of the mineral undoubtedly underlie changes measured in the biomechanical properties of the bones (11, 12). Since bone is a collagen-mineral composite, in which collagen reduces the inherent brittleness of the mineral, one might expect that part of the increased brittleness of oim bone might be attributable to biomechanical changes of collagen. However, to date, no data are available which examine oim collagen mechanical properties. In this context, the tail tendon collagen of the oim mouse is a likely candidate for such investigations since its main component is the same type I collagen comprising bone. Recent x-ray crystallographic investigations of tail tendon collagen from oim mice and controls showed some differences in the lateral molecular packing of the collagen fibrils: The Bragg reflections of a quasi-hexagonal structure superimposed on a broad diffuse scattering, a result which is typical for a liquid-like lateral packing of the molecules, could not be observed (Brodsky, B., personal communication).

In this paper the mechanical behavior of the tail tendon collagen of the oim mouse has been studied. Three different groups of animals were compared in tensile testing of collagen fibers under native wet conditions: the homozygous mutant mouse (oim/oim), the heterozygous mouse (+/oim), and the cross-bred normal mouse (+/+). The consequences of the results obtained for collagen for the biomechanical properties of

Address correspondence to Dr. Peter Fratzl, Ludwig Boltzmann Institut für Osteologie & Institut für Materialphysik, Strudlhofgasse 4, A-1090 Wien, Austria. Phone: 1-31367-3242; FAX: 1-3100183; E-mail: fratzl@pap.univie.ac.at

Received for publication 17 January 1997 and accepted in revised form 28 March 1997.

1. *Abbreviations used in this paper:* OI, osteogenesis imperfecta; oim, osteogenesis imperfecta mouse model.

J. Clin. Invest.

0021-9738/97/07/0040/06 $2.00
Volume 100, Number 1, July 1997, 40–45

bone are then discussed within the framework of a simple model.

Methods

Two oim/oim mutant mice, two +/oim mice, and three +/+ control mice were killed at the age of 14 mo, 14 mo, and 7 mo, respectively. The oim/oim and +/oim mice were all approximately the same weight (26 g), whereas the control mice, which were younger, had a weight of ~ 30 g. The tails of the mice were frozen and stored at ~ −18°C until dissection. At that time, tail tendons were isolated and immediately placed in PBS at pH 7.4. At least nine tendons from each mouse were investigated by mechanical testing at room temperature, some immediately after dissection and others after storage in PBS at 4°C for some days. No change in mechanical data after specimen storage in PBS at 4°C was observed. A small segment was dissected from each tendon and its diameter was measured with a calibrated eyepiece under a light microscope. The remaining part of each tendon was kept in PBS at room temperature to maintain it in a wet condition and mounted into the upper and lower grips of a self-made mechanical testing machine described previously (13).

During testing the entire tendon was immersed in PBS at room temperature. The testing apparatus (grips and container) was made of stainless steel to avoid interaction with PBS. The grips were moved by a motor-driven micrometer stage allowing grip maximum velocity of 0.43 mm/s. The initial distance between the two grips was ~ 13.4 mm before tension was applied to the tendon. For all measurements the velocity of the grips was constant at 0.01 mm/s, corresponding to a strain rate of ~ 0.08%/s. Force measurements were made by using a small load cell directly mounted on the upper grip with a maximal load of 125 N. The minimal measured force of the cell was ~ 0.005 N. Movement of the grips was recorded by an inductive transducer with a resolution of 0.002 mm. Both the signal from the load cell and from the transducer were recorded by a personal computer which also controlled the movement of the grips. Each tendon was stretched to failure and a load–extension curve was recorded. The initial length of each fiber was determined by stretching it until the smallest measurable force (0.005 N) was detected.

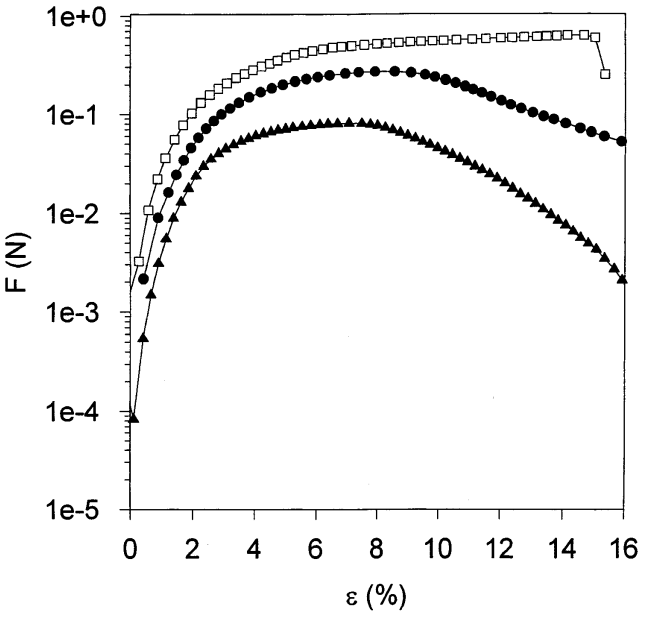

Figure 1. Load–extension curves for typical oim/oim (▲), +/oim (●), and +/+ (□) mice. In this half logarithmic plot, the identical shape of the various curves at low strain (ϵ) is clearly visible, and at intermediate and higher strains the oim/oim mice bear less load than controls at all points. Heterozygous animals fall between mutants and controls.

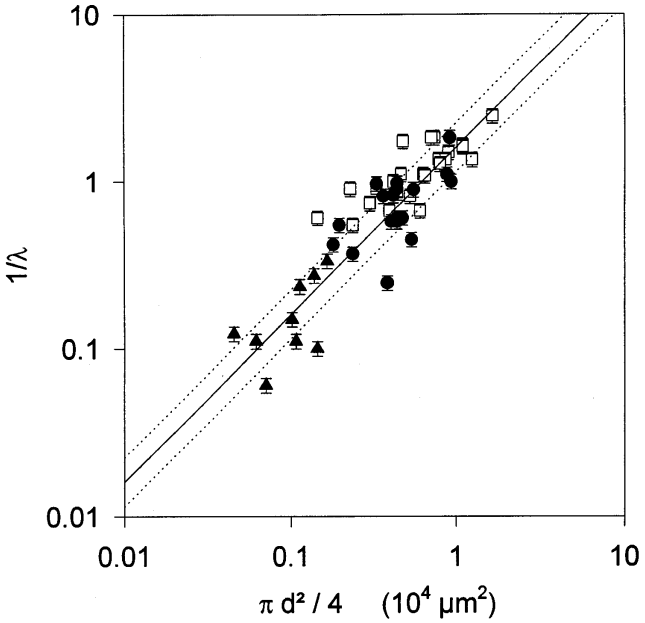

Figure 2. The scaling factor 1/λ plotted as a function of $\pi d^2/4$ where d is the collagen fibril diameter. The solid line has a slope of 1. The dotted lines bracket a deviation of 40% from the solid line. +/+: □; +/oim: ●; oim/oim: ▲.

The applied stress, σ, can be calculated by dividing the measured force, F, by the tendon cross-sectional area, obtained from independent measurements of the diameter, d, of the specimens: Assuming cylindrical symmetry, $\sigma = 4F/(\pi\, d^2)$. With variations in gripping the samples, it was found that the tendon diameter could be measured to an accuracy of only ~ 20%, as was verified by a large number of independent measurements on the same tendon. Because of this uncertainty an alternative method for measuring the applied stress on the specimens was derived as follows. First, the extension of a given tendon was plotted as a function of the logarithm of the measured force. A typical plot of oim/oim, +/oim, and, +/+ tendon samples is shown in Fig. 1. In such plots, the shape of all recorded load/extension data was very similar in the low strain region to about $\epsilon = 5\%$. The curves were shifted in a second step along the vertical axis, corresponding to multiplication of the force, F, by an empirical factor, λ. To achieve a superposition of all curves for strains $\epsilon < 5\%$, the empirical factors thus determined were next plotted in a graph of 1/λ versus tendon collagen cross-sectional area, $\pi d^2/4$, determined by observation in a light microscope (Fig. 2). A large scatter is visible in the data, but the scatter is about the same within each group and consistent with the large errors in the measurement of $\pi d^2/4$ (twice the relative error of d, that is, ~ 40%). A linear regression of the data in Fig. 2 was then used to determine the constant λ_o, so that $\pi d^2/4 = \lambda_o/\lambda$ within the error margins of the direct measurement of d. Errors in the measurements of the diameter, the maximum strain, and maximum stress were determined by ANOVA analysis using a statistical software package SPSS (SPSS Inc., Chicago, IL). Statistical differences between the three groups were considered significant with a confidence interval of 0.99.

Results

In the absence of applied stress, a macroscopic crimp, well known for normal collagen (14), was visible in the fibrils

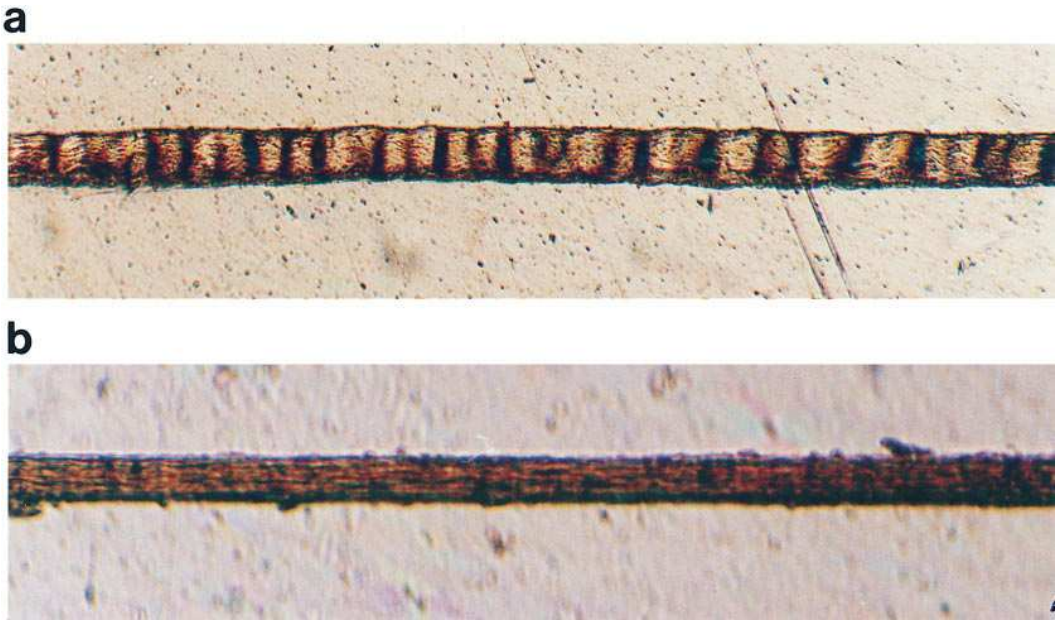

Figure 3. (*a*) The macroscopic crimp of an oim/oim collagen fiber as visualized by polarized light microscopy (14) of an unstretched tail tendon. (*b*) The appearance of the tendon at very low tensile stress. The macroscopic crimp has disappeared. Magnification of the tendon is ×65.

viewed by polarized light microscopy (Fig. 3 *a*) for all three genetic groups and vanished as soon as a stress was applied (Fig. 3 *b*). Typical stress/strain data obtained from measuring one group of oim/oim, +/oim, and +/+ animals are shown in Fig. 4. The stress has been determined from the applied force, F, in the relation $\sigma = \lambda/\lambda_o F$ as explained above. All data exhibited a characteristic shape at low strain, ϵ, which is well recognized for normal type I collagen and usually called the "toe" region of the stress–strain curve (6, 15). No difference was observed in this region (up to $\epsilon = 5\%$) between the three types of animals.

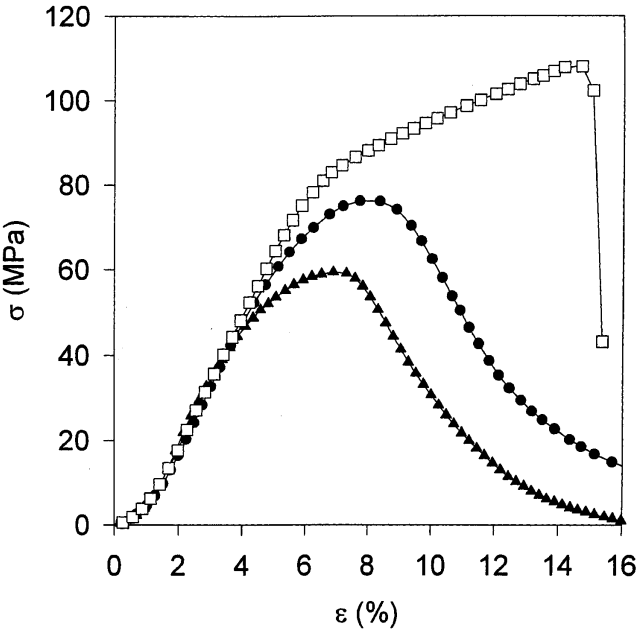

Figure 4. A typical stress (σ)/strain (ϵ) diagram of the tail tendon collagen from oim/oim (▲), +/oim (●), and +/+ (□) animals. The equivalent shape of the curves in the low strain region is apparent. The oim/oim and +/oim collagen have a decreased ultimate stress at increasing strain compared to +/+ collagen. Measurements from +/oim animals fall between those from normal (control) and oim/oim animals.

Over ~ 5%, the stress continued to increase with increasing strain although the modulus (the slope of the curve) became smaller. The stress reached a maximum first for the homozygous mutant (at a strain ~ 6–7%), second for the heterozygotes (at an intermediate strain ~ 8%), and last for the normal animals (typically at 12–16%). This means that the normal collagen can be stretched twice as much as the homozygous mutant before it breaks. It should be noted that the conclusions regarding the strain at maximum stress are not influenced by the normalization of the applied force to stress data (see Methods) since this renormalization only involves a multiplication of the vertical scale by a constant which does not affect the position of the maximum. Even for the maximum stress data (that is, the height of the maximum), the same qualitative results remained true regardless of which of the two methods was used to determine the stress σ (see Methods).

Fig. 5, *a*, *b,* and *c*, summarize mean tendon collagen diameter, strain at maximum stress, and maximum stress for oim/oim, +/oim, and +/+ animals. Fig. 5 *a* shows that the average diameter of collagen in oim/oim mice is significantly smaller than the average diameter of the other groups (a confidence interval of 0.99 was considered significant). This is true even though the normal control mice were younger and the tendon diameter is known to increase with age. Measured strain at maximum stress and the maximum stress itself were significantly larger for normal (+/+) compared to either +/oim or oim/oim mice.

Discussion

Tail tendons from oim mice were found to be mechanically weaker than normal counterparts because, first, their cross-sectional areas were significantly smaller. By scaling the load–extension curves to stress–strain diagrams, the experiments re-

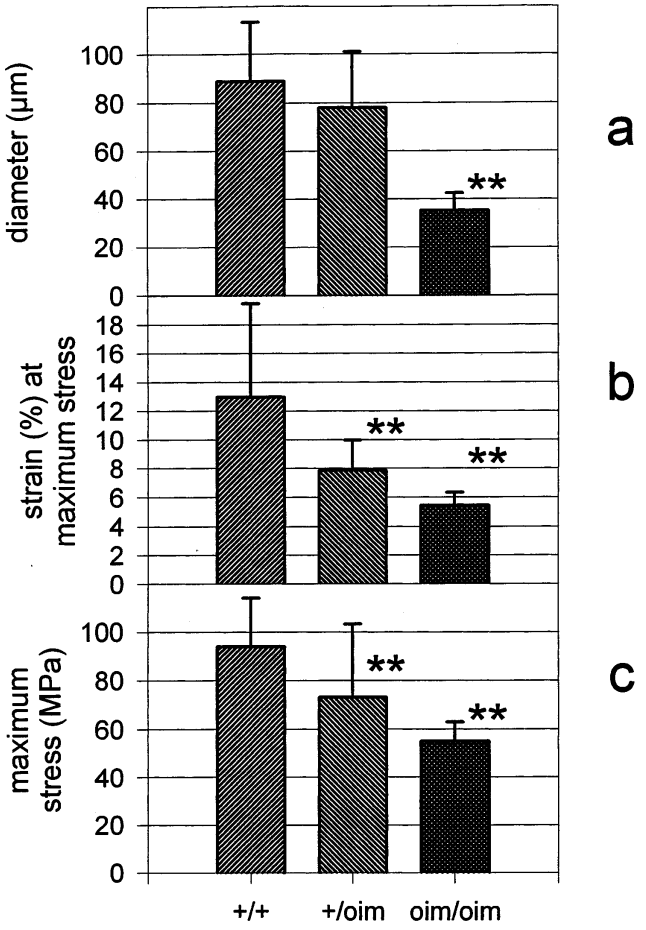

Figure 5. Average measurements of the diameter of tail tendon collagen fibers, the average strain at maximum stress, and average maximum stress for +/+ ($n = 25$), +/oim ($n = 18$), and oim/oim ($n = 9$) mice. *n*, number of fibers investigated. The error bars represent one standard deviation of the mean, and asterisks indicate significant differences compared to controls with a confidence interval of 99% (by analysis of variance).

vealed, second, a dramatic change in ultimate stress and strain data for the oim/oim compared to control animals, in agreement with recent measurements (16). At small strains the curves were nearly identical for all genotypes. This finding at small strains appears to correspond to the stretching of a characteristic macroscopic crimp commonly observed in tendon and found here to be present in all mice examined.

At strain levels $> 5\%$ and near the points of ultimate stress and strain, significant differences between oim/oim and +/+ mice occur. It may be here that, related to normal cross-links and structure, collagen molecules slide with respect to each other and/or stretch to compensate for their undergoing mechanical forces (17–19). On the other hand, in the absence of $\alpha 2$(I) chains in the mutant, the oim/oim mouse may suffer from a different type or number of a cross-link or abnormal cross-links altogether. In this case, one may speculate that critical bonds are missing or that certain bonds, possibly of a covalent nature, which could be either intra- or interchain protein bonds, may be breaking prematurely in oim/oim collagen to account for the stress–strain curves generated here. In the same context, such putatively different, absent, or altered bonds may yield a collagen molecular assemblage similar to that proposed recently on the basis of electron microscopic tomography of the unusually mineralized leg tendons from oim mice (20, 21). Indeed, poorly aligned collagen hole and overlap zones and resultant discontinuous hole zone channels suggested by such studies (20, 21) may occur by a changing nature of the chemical bonds in the mouse mutant. Further investigations of the cross-linking or other chemical structure and organization of oim collagen would be required to clarify this possibility.

Regardless of the exact underlying cause, it is clear that the mutant animals have a reduced tensile strength of their collagen alone. Such a change will undoubtedly have consequences on the mechanical properties of oim bone. The lower maximum stress and strain of bone collagen fibers could conceivably be the source of increased brittleness of the oim mouse bone.

A schematic model of mineralized collagen, shown in Fig. 6, provides some insight into the relation between collagen structure and tensile force (adapted from reference 22). The upper part shows an unmineralized normal collagen fibril, the constituent collagen molecules being assembled in a 67 nm stagger, the periodicity composed of adjacent gap (hole) and overlap regions in the usual way (23). Mineral crystals are first nucleated principally in the hole zones and also in overlap regions of the collagen fibrils and once nucleated the crystals grow in the same locations (24–27). The second part of Fig. 6 shows holes filled with mineral crystals (plates or needles) viewed edge-on in the figure. A similar schematic could be made for unmineralized and mineralized oim collagen, the ultrastructure, assembly, and organization of which has been described recently (20, 21). The thickness of the incipient crystals (that is, their smallest dimension) has been consistently found in the order of 2–4 nm for most types of bone (11, 22, 27, 28). In particular, for young oim/oim mice and oim/+ animals, this dimension was ~ 2 nm (12). It is important to realize that the presence of a crystal of this dimension in a hole between two normal or oim collagen molecules will result in a significant local distortion of the molecules and, hence, a tensile force on the molecules will be exerted. The distortion and forces placed on a molecule are schematically illustrated in the lower part of Fig. 6.

Under normal conditions, the tensile force on the molecules can be expected to improve the mechanical properties of bone (22) since it creates a compressive stress onto the hard mineral, which can support high compressive but much smaller tensile loads (the ultimate strain of the mineral is $\sim 0.1\%$ strain [6]). Indeed, recent investigations of the relation between mechanical properties of tendon and mineral content showed that with increasing mineral content the ultimate stress increases by a factor of three (19). On the other hand, the ultimate strain is only about one-third of the value for unmineralized tendon (19). Another effect is that mineralization reduces the average lateral distance between collagen molecules (20, 21, 29), a result which increases their direct interaction and probably reduces their capability of gliding and thus accommodating tensile stresses.

Assuming that mineral crystals have nucleated and grown into oim collagen fibrils in a similar way, the oim collagen must be increasingly prestrained with increasing mineral content. Since the ultimate strain of the oim collagen decreases from

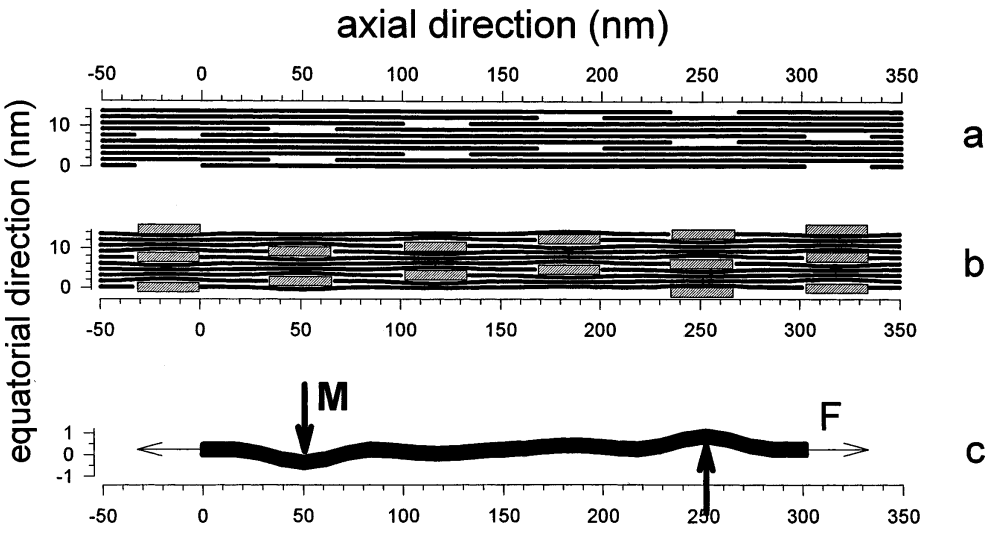

Figure 6. Schematic diagram of normally mineralized collagen (adapted from reference 22). The upper part of the diagram shows collagen molecules assembled normally with an axial period of 67 nm. The typical separation of the molecules in the equatorial direction is on the order of 1.5 nm. As shown in the middle part of the diagram, when mineral crystals (plates or needles) grow with a thickness > 1.5 nm in the collagen hole zones, a distortion of the collagen molecules must occur which increases as the crystals become thicker. A schematic path of one molecule of the four located between hole zones is shown in the lower part of the diagram. M indicates the distortion induced by a growing mineral crystal and F indicates the resulting tensile force on the molecule.

~ 12 to $\sim 6\%$ as demonstrated in this study, it should be expected that oim collagen will have no further capability of extending when the bone is submitted to large external tensile forces. Hence, oim collagen will fail and so will the mineral, which itself is naturally brittle. As a consequence, oim/oim bone tissue can be expected to be brittle as a whole. When the same external forces are applied to normal bone, the mineral may not resist the tensile strain, but the normal collagen would be able to accommodate these strains further without failure and to take up some deformation energy. Therefore, under the same conditions in which oim/oim bone fractures, normal bone can be expected not to break.

In addition to the present data showing reduced tensile stress supported by collagen, smaller and less well-aligned mineral crystals have been found previously in the oim mouse model (12). Since the effective pretensioning of the collagen will depend on the thickness of mineral crystals (see Fig. 6) and the thickness is known to increase with age in normal tissue (22), one might speculate that crystal growth inside collagen fibrils could be limited by a strongly reduced maximum tension in oim collagen since continuous growth of the crystals (thickness and other dimensions) would ultimately result in damage to the collagen fibrils. Within a damaged collagen matrix, a less constrained growth of mineral crystals could possibly lead to the large blocklike crystals also reported in oim bone (20). Although to date there is no proof for these effects, they could be an attractive explanation for the coexistence of large blocklike mineral crystals and others with reduced thickness as compared to normal bone.

In conclusion, this study suggests that the brittleness of bone in the oim mouse resides in part in a strongly reduced maximum stress and strain that can be attributed to the major protein of the tissue, collagen. This in turn may be the consequence of the absence of the $\alpha 2$(I) chain of collagen in this mouse mutant and, if so, it suggests that this constituent plays a specific and important role in cross-linking and therefore in providing tensile strength and mechanical integrity to a vertebrate connective or mineralized tissue.

Further investigations, such as x-ray scattering measurements of the collagen structure at definite strains, should be performed in the future to expand this hypothesis. Indeed, additional information on the structure and mechanical properties of the "soft" part of the collagen/mineral composite in bone appears to be crucial for a better understanding of the OI disease not only in the mouse mutant but also in human pathologies.

Acknowledgments

The authors are grateful to Dr. H. Peterlik (Institut für Materialphysik der Universität Wien, Wien) and to Dr. B. Brodsky (Department of Biochemistry, University of Medicine and Dentistry of New Jersey, Piscataway, NJ) for valuable discussions.

W.J. Landis was supported by grant AR-41452 from the National Institutes of Health.

References

1. Traub, W., T. Arad, U. Vetter, and S. Weiner. 1994. Ultrastructural studies of bones from patients with osteogenesis imperfecta. *Matrix Biol.* 14:337–345.

2. Prockop, D.J. 1992. Mutations in collagen genes as a cause of connective-tissue diseases. *N. Engl. J. Med.* 326:540–546.

3. Smith, R., M.J.O. Francis, and G.R. Houghton. 1983. The Brittle Bone Syndrome: Osteogenesis Imperfecta. Butterworth, London: 74–82.

4. Sillence, D.O., A. Senn, and M.D. Danks. 1979. Genetic heterogeneity in osteogenesis imperfecta. *J. Med. Genet.* 16:101–116.

5. Vetter, U., B. Pontz, E. Zauner, R.E. Brenner, and J. Sprangerl. 1992. Osteogenesis imperfecta: a clinical study of the first ten years of life. *Calcif. Tissue Int.* 50:36–41.

6. Vincent, J. 1990. Structural Biomaterials. Princeton University Press, New York. 183–185.

7. Vetter, U., M.A. Weis, M. Mörike, E.D. Eanes, and D.R. Eyre. 1993. Collagen crosslinks and mineral crystallinity in bone of patients with osteogenesis imperfecta. *J. Bone Miner. Res.* 8:133–137.

8. Cassella, J.P., and S.Y. Ali. 1992. Abnormal collagen and mineral formation in osteogenesis imperfecta. *Bone Miner.* 17:123–128.

9. Chipman, S.D., H.O. Sweet, D.J. McBride, Jr., M.T. Davisson, S.C. Marks, Jr., A.R. Shuldiner, R.J. Wenstrup, D.W. Rowe, and J.R. Shapiro. 1993. Defective proα2(I) collagen synthesis in a new recessive mutation of mice: a model of human osteogenesis imperfecta. *Proc. Natl. Acad. Sci. USA.* 90:1701–1705.

10. Prockop, D.J., A. Colige, H. Helminen, J.S. Khillan, R. Pereira, and Ph. Vandenberg. 1993. Mutations in type I procollagen that cause osteogenesis imperfecta: effects of the mutations on the assembly of collagen into fibrils, the basis of phenotypic variations, and potential antisense therapies. *J. Bone Miner. Res.* 8:489–492.

11. Fratzl, P., S. Schreiber, and K. Klaushofer. 1996. Bone mineralization as studied by small-angle x-ray scattering. *Connect. Tissue Res.* 34: 247–254.

12. Fratzl, P., O. Paris, K. Klaushofer, and W.J. Landis. 1996. Bone mineralization in an osteogenesis imperfecta mouse model studied by small-angle x-ray scattering. *J. Clin. Invest.* 97:396–403.

13. Misof, K., G. Rapp, and P. Fratzl. 1996. A new molecular model for collagen elasticity based on synchrotron x-ray scattering evidence. *Biophys. J.* 72: 1376–1381.

14. Diamant, J., A. Keller, E. Baer, M. Litt, and R.G.C. Arridge. 1972. Collagen: Ultrastructure and its relation to mechanical properties as a function of aging. *Proc. R. Soc. Lond. B. Biol. Sci.* 180:293–315.

15. Silver, F.H., Y.P. Kato, M. Ohno, and A.J. Wasserman. 1992. Analysis of mammalian connective tissue: relationship between hierarchical structures and mechanical properties. *Journal of Long-Term Effects of Medical Implants.* 2:165–195.

16. McBride, D.J., N.S. Fedarko, J.R. Shapiro, and M.G. Dunn. 1996. The proα2(I) chain improves the mechanical performance of type I collagen. American Society of Bone Mineral Research 18th Annual Meeting. M453:S295. (Abstr.)

17. Folkhard, W., E. Mosler, W. Geercken, E. Knörzer, H. Nemetschek-Gansler, and T. Nemetschek. 1986. Quantitative analysis of the molecular sliding mechanism in native tendon collagen–time-resolved dynamic studies using synchrotron radiation. *Int. J. Biol. Macromol.* 9:169–175.

18. Mosler, E., W. Folkhard, E. Knörzer, H. Nemetschek-Gansler, T. Nemetschek, and M.H.J. Koch. 1985. Stress-induced molecular rearrangement in tendon collagen. *J. Mol. Biol.* 182:589–596.

19. Landis, W.J., J.J. Librizzi, M.G. Dunn, and F.H. Silver. 1995. A study of the relationship between mineral content and mechanical properties of turkey gastrocnemius tendon. *J. Bone Miner. Res.* 10:859–867.

20. Landis, W.J. 1995. Tomographic imaging of collagen-mineral interaction: implications for osteogenesis imperfecta. *Connect. Tissue Res.* 31:287–290.

21. Landis, W.J. 1995. The strength of a calcified tissue depends in part on the molecular structure and organization of its constituent mineral crystals in their organic matrix. *Bone (N.Y.).* 16:533–544.

22. Fratzl, P., N. Fratzl-Zelman, K. Klaushofer, G. Vogl, and K. Koller. 1991. Nucleation and growth of mineral crystals in bone studied by SAXS. *Calcif. Tissue Int.* 48:407–413.

23. Hodge, A.J., and J.A. Petruska. 1963. Recent studies with the electron microscope on ordered aggregates of the tropocollagen molecule. *In* Aspects of Protein Structure. G.N. Ramachandran, editor. Academic Press, New York. 289–300.

24. Veis, A.S., and B. Sabsay. 1987. The collagen of mineralized matrices. *Bone Miner. Res.* 5:1–63.

25. Glimcher, M.J. 1976. Composition, structure and organization of bone and other mineralized tissues and the mechanism of calcification. *In* Handbook of Physiology-Endocrinology, Vol. 7. R.O. Greep and E.B. Astwood, editors. American Physiological Society. Washington, DC. 25–116.

26. Landis, W.J., M.J. Song, A. Leith, L. McEwen, and B. McEwen. 1993. Mineral and organic matrix interaction in normally calcifying tendon visualized in three dimensions by high-voltage electron microscopic tomography and graphic image reconstruction. *J. Struct. Biol.* 110:39–54.

27. Lees, S., L.C. Bonar, and H.A. Mook. 1984. A study of dense mineralized tissue by neutron diffraction. *Int. J. Biol. Macromol.* 6:321–326.

28. Fratzl, P., N. Fratzl-Zelman, and K. Klaushofer. 1993. Collagen packing and mineralization: an x-ray scattering investigation of turkey leg tendon. *Biophys. J.* 64:260–266.

29. Lees, S. 1987. Considerations regarding the structure of the mammalian mineralized osteoid from the viewpoint of the generalized packing model. *Connect. Tissue Res.* 16:281–303.